

Response of *Burkholderia cenocepacia* H111 to Micro-Oxia

Gabriella Pessi^{1*}, Rubina Braunwalder¹, Alexander Grunau¹, Ulrich Omasits², Christian H. Ahrens², Leo Eberl¹

¹ Department of Microbiology, University of Zurich, Zürich, Switzerland, ² Institute of Molecular Life Sciences, University of Zurich, Zürich, Switzerland

Abstract

B. cenocepacia is an opportunistic human pathogen that is particularly problematic for patients suffering from cystic fibrosis (CF). In the CF lung bacteria grow to high densities within the viscous mucus that is limited in oxygen. *Pseudomonas aeruginosa*, the dominant pathogen in CF patients, is known to grow and survive under oxygen-limited to anaerobic conditions by using micro-oxic respiration, denitrification and fermentative pathways. In contrast, inspection of the genome sequences of available *B. cenocepacia* strains suggested that *B. cenocepacia* is an obligate aerobic and non-fermenting bacterium. In accordance with the bioinformatics analysis we observed that *B. cenocepacia* H111 is able to grow with as little as 0.1% O₂ but not under strictly anoxic conditions. Phenotypic analyses revealed that H111 produced larger amounts of biofilm, pellicle and proteases under micro-oxic conditions (0.5%–5% O₂, i.e. conditions that mimic those encountered in CF lung infection), and was more resistant to several antibiotics. RNA-Seq and shotgun proteomics analyses of cultures of *B. cenocepacia* H111 grown under micro-oxic and aerobic conditions showed up-regulation of genes involved in the synthesis of the exopolysaccharide (EPS) cepacian as well as several proteases, two isocitrate lyases and other genes potentially important for life in micro-oxia. Data deposition: RNA-Seq raw data files are accessible through the GEO Series accession number GSE48585. MS data have been deposited in the ProteomeXchange database (PXD000270).

Citation: Pessi G, Braunwalder R, Grunau A, Omasits U, Ahrens CH, et al. (2013) Response of *Burkholderia cenocepacia* H111 to Micro-Oxia. PLoS ONE 8(9): e72939. doi:10.1371/journal.pone.0072939

Editor: Tom Coenye, Ghent University, Belgium

Received: May 30, 2013; **Accepted:** July 15, 2013; **Published:** September 2, 2013

Copyright: © 2013 Pessi et al. This is an open-access article distributed under the terms of the Creative Commons Attribution License, which permits unrestricted use, distribution, and reproduction in any medium, provided the original author and source are credited.

Funding: This work was financially supported by the Swiss National Science Foundation (Project 31003A-143773) to LE and the Swiss SystemsX.ch initiative (grant IPP 2011/121) to CHA and LE. The funders had no role in study design, data collection and analysis, decision to publish, or preparation of the manuscript.

Competing Interests: The authors have declared that no competing interests exist.

* E-mail: gabriella.pessi@botinst.uzh.ch

Introduction

Burkholderia cenocepacia is one of the 17 members of the *Burkholderia cepacia* complex (Bcc) whose extraordinary metabolic versatility allows it to adapt to a variety of environmental conditions, including infection sites in humans [1,2]. Of particular concern are lung infections of patients suffering from cystic fibrosis (CF). One of the major problems associated with Bcc infections is their capacity to form highly organized surfaced-associated communities (biofilms) with an intrinsic resistance to most common antibiotics in clinical use [1,3]. Several strains of the Bcc species *B. multivorans*, *B. cenocepacia*, *B. cepacia*, and *B. dolosa* have been shown to be highly transmissible between patients [4], with *B. cenocepacia* and *B. multivorans* accounting for the majority of CF infections [5]. During chronic colonization of the CF lung, bacteria are under strong selective pressures that result from challenges of the immune defense, antimicrobial therapy, nutrient and oxygen availability [6]. *B. cenocepacia* produces biofilms and uses the highly viscous mucus of the CF lung as a rich nutrient source. Due to bacterial respiration a steep oxygen gradient within the mucus is generated and the deeper layers become anaerobic [7–10]. This observation is supported by the fact that anaerobes have been found to occur in CF sputum at high cell densities [11]. Recently, Alvarez-Ortega and colleagues provided evidence that the major CF pathogen *P. aeruginosa* is growing in the CF lung preferentially by micro-oxic respiration [12]. Moreover, chemostat

experiments with aerobic and micro-oxic cultures of *P. aeruginosa* suggested that this facultative anaerobe is growing optimally in a micro-oxic environment where it is producing more virulence factors such as the exopolysaccharide (EPS) alginate and pyocyanine [13]. Further studies have also shown that an anaerobic environment stimulates the production of alginate [7,9]. In anaerobiosis, *P. aeruginosa* can utilize nitrate or nitrite rather than oxygen as a terminal electron acceptor [14–17]. In the absence of nitrate or nitrite, it can convert arginine to ornithine, thereby generating energy for anoxic growth [16–18]. Finally *P. aeruginosa* can use pyruvate fermentation for long-term survival of up to 18 days under anoxic conditions and this conversion of pyruvate into lactate, acetate, and succinate is in turn inhibited by nitrate respiration [19].

In a retrospective study of a *Burkholderia dolosa* outbreak among CF patients, the genomes of 112 isolates collected from 14 individuals over 16 years were sequenced and intriguingly revealed that 3 out of the 17 genes found to be under strong selection during pathogenesis had mutations in genes involved in oxygen-dependent regulation [20]. This suggests that sensing of a low oxygen environment is critical for pathogenesis in lung infections.

These findings posed the question of how *B. cenocepacia*, which is considered an obligate aerobe, can grow or survive in the micro-oxic/anoxic CF lung environment. Very recently, Sass and colleagues reported a low-oxygen activated locus (*lxa*) that has been shown to play an important role in regulation of the low

oxygen response in *B. cenocepacia* strains J2315 and K56-2 [21]. After exposure to an anoxic environment, the *lxa* mutant showed less viable cells compared to the wild type. However, the *B. cenocepacia* H111 strain, which was originally isolated from a CF patient as well as other *B. cepacia* complex (Bcc) strains, do not possess the *lxa* locus [21,22].

Here we show that *B. cenocepacia* H111 as well as other *B. cenocepacia* strains did not display any obvious functions that would allow anaerobic growth: no genes were found that are involved in denitrification and arginine fermentation. However, H111 is able to grow at an oxygen concentration of 0.1%, yet cannot grow anoxically in culture. When grown micro-oxically, *B. cenocepacia* produces more substratum-associated biofilm mass as well as a more robust pellicle compared to aerobic conditions. Finally, RNA-Seq and shotgun proteomics analyses from matched aerobic and micro-oxic samples were carried out to obtain a more detailed view of the repertoire of genes and proteins potentially important for growth in a low oxygen environment.

Results

Growth of *B. cenocepacia* H111 at different oxygen concentrations

The ability of *B. cenocepacia* to grow at different oxygen concentrations in complex media was tested. When cells were grown under normal aerobic conditions (21% O₂), the cells grew to an optical density (OD₆₀₀) of around 3 with a generation time of approximately 65 minutes. When only 5% or 0.5% oxygen was supplied (see Methods), the cells grew slower (generation times of 113 and 180 minutes, respectively), probably because the dissolved oxygen concentration dropped quickly to growth limiting levels (Figure 1). However, *B. cenocepacia* was still able to grow with 0.1% oxygen with a doubling time of 268 minutes, reaching an OD₆₀₀ of 0.7. To test for growth in the absence of oxygen, several alternative electron acceptors, including nitrate, fumarate, and DMSO as well as the C-sources pyruvate, oxalate and arginine and a medium mimicking synthetic mucus [12], were tested.

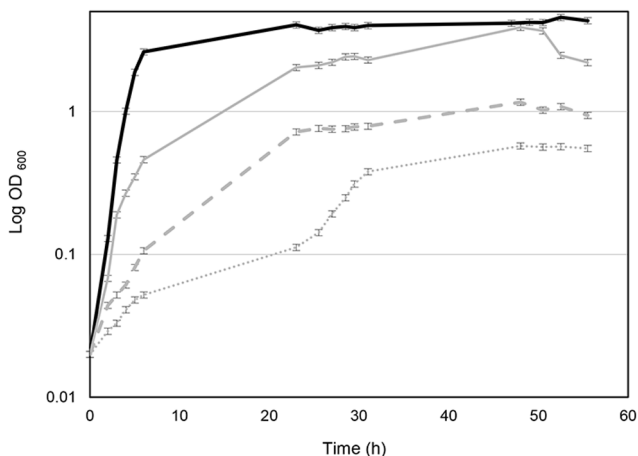


Figure 1. Growth of *B. cenocepacia* at different oxygen concentrations (21%, 5%, 0.5% and 0.1%). Aerobic cultures (21%, black line) were grown with shaking in 1L Erlenmeyer flasks containing 100 ml LB medium while micro-oxic cultures were grown in 500-ml rubber-stoppered serum bottles containing 25 ml LB medium in presence of a nitrogen gas atmosphere that contained 5% (grey line), 0.5% (grey dashed line) or 0.1% (grey dotted line) oxygen (Pangas). Whiskers indicate SD, n=3.

doi:10.1371/journal.pone.0072939.g001

However, in none of the conditions tested did we observe growth in the absence of oxygen.

Identification of genes in the *B. cenocepacia* H111 genome that may be required for growth under “low-oxygen” conditions

To identify genes related to denitrification, arginine fermentation or pyruvate fermentation, we searched for the corresponding *P. aeruginosa* orthologs in *B. cenocepacia* H111 and other sequenced *Burkholderia* species. The genes required for denitrification which encode all enzymes for nitrate/nitrite, nitric-oxide and nitrous-oxide reduction (PA3872-75, PA0509-PA0519, PA0520-24, PA3391-96), could only be identified in the “pseudomallei” group members *B. thailandensis*, *B. pseudomallei* and *B. mallei*. Indeed *B. pseudomallei* was reported to be able to survive without oxygen using nitrate respiration [23,24]. In contrast, *B. cenocepacia* strains, including strain H111 were found to only possess the nitrite reductase encoding gene cluster (BCAM1683-86). *P. aeruginosa* is also able to generate ATP by the degradation of arginine to ornithine, which requires expression of the *arcABC* operon (PA5170-73) [18]. While *arcB* (ornithine carbamoyltransferase) is present in all sequenced *B. cenocepacia* strains, the entire operon is only present in strains of *B. thailandensis*, *B. pseudomallei*, *B. mallei*, *B. ambifaria*, *B. xenovorans*, *B. phymatum* and *B. phytofirmans*. The fermentation of pyruvate can also be used by *P. aeruginosa* to generate energy and survive during anoxic growth (PA0835-36 and PA0927) [19]. The genes necessary for the conversion of pyruvate to lactate, acetate, and succinate, i.e. the acetate kinase *ackA*, the phosphate acetyltransferase *pta* and the lactate dehydrogenase *ldhA*, were found in the genome of all *Burkholderia* species. Many bacteria adapt to micro-oxic conditions by synthesizing a particular cytochrome c oxidase (*cbb3*) complex with a high affinity for oxygen [25–27]. No classical *cbb3* cytochrome oxidase was found in any of the sequenced *Burkholderia* strains. In contrast, a homolog of the *bd*-type oxidase (cyanide insensitive) was identified in the genome of several *Burkholderia* strains including strain H111 (BCAM2674-75). Homologs of the *P. aeruginosa* central regulator of anaerobic metabolism FNR/ANR (PA1544) [28] were identified in all sequenced *Burkholderia* strains. The strain H111 has two FNR/ANR orthologs, BCAM0049 and BCAM1483.

Micro-oxic conditions favor the sessile lifestyle

The capacity of our model strain H111 to form a biofilm in a polystyrene microtiter dish-based assay was tested under aerobic and micro-oxic conditions. The biofilm index (BI), i.e. biofilm mass normalized against planktonic growth, was used to compensate for the different growth rates. The amount of adhered biomass in cells grown to the begin of stationary phase was found to be significantly higher with 0.5% oxygen (Biofilm Index 80%) compared to 21% oxygen (Biofilm index 55%) (p-value<0.01, Figure 2). We also tested for pellicle formation, i.e. the biofilm formed at the liquid-air interface of static cultures and *B. cenocepacia* was found to produce more pellicle under micro-oxic conditions (data not shown). Other phenotypes such as swarming and swimming motility were not affected by oxygen availability after 48 hours of incubation. In contrast, the production of siderophores as measured on CAS plates was reduced in micro-oxically grown cells (Figure S1).

The production of extracellular factors such as cellulases, proteases, lipases, was also investigated. These assays revealed that proteolytic activity was significantly higher under micro-oxic conditions (p-value<0.01, Figure 3) while lipolytic and cellulolytic

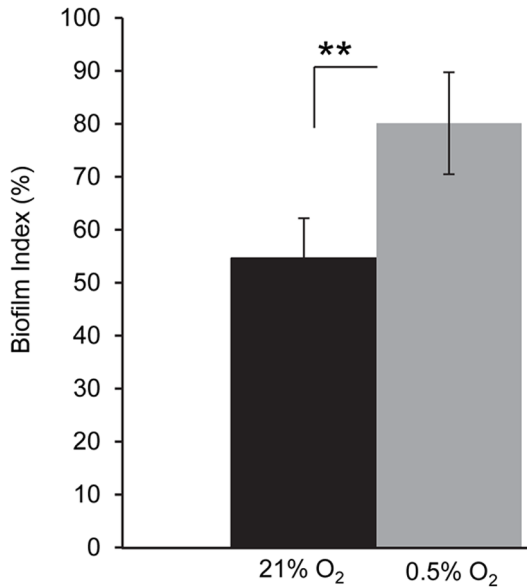


Figure 2. Influence of oxygen on biofilm formation in *B. cenocepacia* H111. Biofilm formation in ABC minimal medium. *B. cenocepacia* H111 was grown in 96-well plates under aerobic (black) or in micro-oxic (grey) conditions created in a CampyGen compact system (oxid). Whiskers indicate SD, n = 3. doi:10.1371/journal.pone.0072939.g002

activities remained constant and were independent of the oxygen level. To examine whether cells that were grown with low oxygen were also more resistant to antibiotics, we exposed cells grown micro-oxically and aerobically on plates to the aminoglycosides kanamycin, gentamycin and to tetracycline. Cells grown micro-oxically showed an increased resistance to all tested aminoglycosides as well as to tetracycline (Figure 4).

Oxygen availability affects metabolic pathways

The metabolism of *B. cenocepacia* H111 grown under aerobic and micro-oxic conditions was compared using Biolog plates for carbon (C) and nitrogen (N) utilization. In these assays the strain's ability to oxidize 190 carbon and 95 nitrogen substrates was tested. An overview of all significant differences in C and N-source utilization under aerobic versus micro-oxic conditions is presented

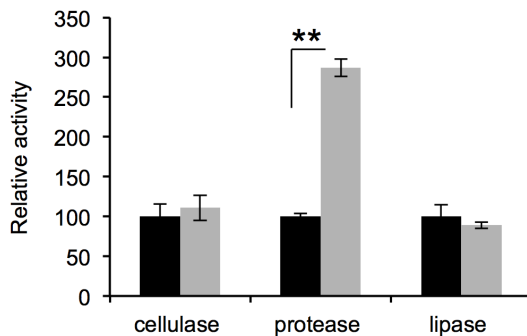


Figure 3. Protease activity is increased in micro-oxia. The exoenzymes cellulase, protease and lipase were measured in supernatants of aerobic (black) and micro-oxic (grey) growing cells as described in material and methods. The activity in the supernatant of aerobic cells was set to 100%. Whiskers indicate SD, n = 6. doi:10.1371/journal.pone.0072939.g003

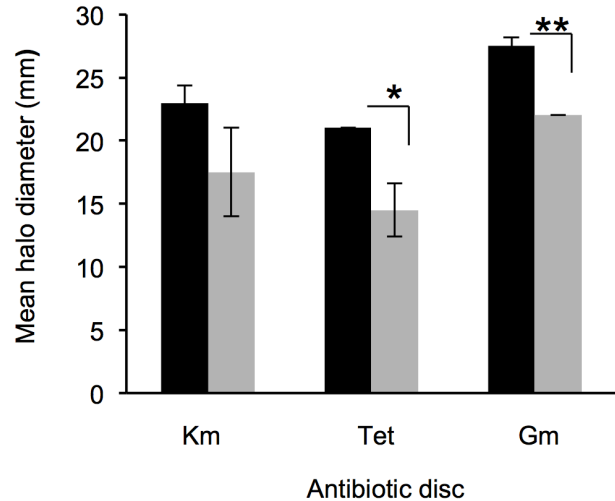


Figure 4. Oxygen-dependent antibiotic resistance profile of *B. cenocepacia* H111. Discs containing 30 µg Kanamycin, 30 µg Tetracycline or 10 µg Gentamycin, respectively, were placed on a plate containing *B. cenocepacia* H111 strain. Plates were incubated aerobically (black) or micro-oxically (grey) and mean halo diameters were determined. Whiskers indicate SD, n = 3. doi:10.1371/journal.pone.0072939.g004

in Table 1. Interestingly, H111 was able to metabolize approximately 70% of the tested C- sources and around 90% of the investigated N-sources. We observed that micro-oxic cells grew to a 4-fold higher optical density (OD₆₀₀) on inosine and to a 2-fold greater OD on adenosine, tricarballic acid, malonic acid and succinamic acid compared to aerobically growing cells. For the utilization of N-sources we found a 2-fold increased respiration of ethylenediamine and D, L-α- amino-caprylic acid under micro-oxia.

Global transcript and protein expression changes in response to low oxygen

To investigate the underlying molecular mechanisms of the observed phenotypic alterations under micro-oxic conditions we performed a transcriptomic as well as a proteomic analysis. For a global profiling of transcript and protein levels, aerobic and micro-oxic cells were grown to the late exponential phase (OD₆₀₀ of 0.8 and 0.4, respectively, Figure 1). Total protein extracts and RNA were obtained from matched samples and further processed (see Methods). To enable detection of low abundance proteins, samples were subfractionated and analyzed using an exclusion list approach [29]. The analysis of cytoplasmic, extracellular and membrane fractions identified a total of 2128 proteins (1726 in oxia, 1911 in micro-oxia). We used DESeq [30] to generate a list of differentially expressed proteins (or genes, see below), ranked according to statistical significance (see Methods). Of the top 58 differentially expressed proteins (Figure 5) the majority (41) were up-regulated in micro-oxia. A global transcript profile analysis of the same samples identified 3806 and 4133 genes expressed aerobically and micro-oxically, respectively. Of the 123 top differentially expressed genes identified by DESeq, 102 were up-regulated in micro-oxia. Importantly, of the 58 differentially expressed proteins, 51 were also found to be similarly regulated at the transcript level. Altogether, we obtained a list of 176 genes and/or proteins that were differentially regulated by low-oxygen (Table 2). Among them, 139 genes/proteins (78%) were up-regulated in micro-oxia, including several transporters

Table 1. List of carbon- and nitrogen compounds that were differentially used in micro-oxic versus aerobic conditions.

Plates	Aerobiosis		Micro-oxia	
	3×increased	2×increased	4×increased	2×increased
C-source	Glycyl-L-aspartic acid	α -hydroxy glutaric acid- γ lactone	Inosine	Adenosine
		Propionic acid		Tricarballic acid
		2-hydroxy benzoic acid		Malonic acid
		β -hydroxy butyric acid		2-deoxy-D-ribose
N-source		L-Lysine		Succinamic acid
		Alloxan		Ethylendiamine
		D-glucosamine		D,L- α -amino-caprylic acid
		Guanine		
		Agmatine		

Biolog plates PM1 and PM2a were used for C-source profiling and plate PM3b for N-sources utilization.
doi:10.1371/journal.pone.0072939.t001

(BCAL0447, BCAS0081, BCAS0451, BCAS0602) and outer membrane proteins, genes involved in synthesis of the EPS cepacian (BCAM1004-1005 and BCAM1010), several proteases (Table 2) and an isocitrate lyase (ICL, BCAL2118). Several genes/proteins involved in reactive oxygen species (ROS) scavenging such as catalases, the alkyl hydroperoxide reductase AhpC and several thioredoxins showed increased expression in low-oxygen conditions. Among the highly up-regulated transcriptional regulators was the FNR-type regulator BCAM0049 as well as the *rpoS* homolog BCAM1259. A functional classification based on proNOG categories of the EggNOG resource [31] (see Methods) revealed that genes/proteins involved in post-translational modification, protein turnover and chaperones (category O) are over-represented in the list of genes/proteins that are up-regulated by low oxygen. In contrast, the functional categories “cell motility (category N)” and “inorganic ion transport and metabolism (category P)” are enriched in the dataset of genes/proteins down-regulated in micro-oxia.

To further validate the global analysis data, the up-regulation of several genes was confirmed by qPCR (Table S3). These included up-regulation of *BCAM0049* and *BCAM1259* expression as well as increased expression of the protease gene *BCAL1919* (*clpB*), the cytochrome d ubiquinol kinase gene *BCAL0785*, the sugar transferase gene involved in cepacian synthesis (*BCAM1010*) and the ICL encoding gene (*BCAL2118*). In addition, transcriptional *lacZ* fusions to promoter regions of selected genes up-regulated in micro-oxic conditions were constructed and measured (Figure S2). The promoter of a gene involved in cepacian biosynthesis (sugar transferase *wcaJ*), the thioredoxin *BCAL2780*, the *rpoS* homolog (*BCAM1259*) and the lectin encoding gene *BCAM0185* showed increased activity when cells were grown with low oxygen (Figure S2). As a control we used $P_{cepI-lacZ}$ transcriptional fusion and confirmed that the expression of the AHL encoding gene *cepI* was not affected by oxygen availability (confirming our RNA-Seq data).

Discussion

At present very little is known of how *B. cenocepacia* strains can adapt to the micro-oxic/anoxic environment within biofilms in the CF lung [7–9,32]. While the CF pathogen *P. aeruginosa* uses denitrification and fermentation of arginine to generate energy for growth and survival in an environment depleted of oxygen [16,17], we could only detect very few orthologs of the respective

genes involved in these processes in the genomes of *B. cenocepacia* strains. Denitrification genes were exclusively found in the genomes of members of the “pseudomallei” group, namely *B. thailandensis*, *B. pseudomallei* and *B. mallei*. Only strains of *B. thailandensis*, *B. pseudomallei*, *B. mallei*, *B. ambifaria*, *B. xenovorans*, *B. phymatum* and *B. phytofirmans*, harbor genes that potentially allow these species to ferment arginine to gain energy (1 mol of ATP per mol of arginine). In accordance with these findings it has been reported that the diversity of *Burkholderia* strains growing under anoxic conditions in soils is very low [33].

The facultative intracellular pathogen *Mycobacterium tuberculosis* has recently been shown to adapt to and recover from hypoxia using isocitrate lyase (ICL)-mediated production of succinate [34]. ICL is a glyoxylate shunt enzyme, which generates succinate whose secretion was proposed to help maintain membrane potential and ATP synthesis. The produced succinate is also a substrate of the succinate dehydrogenase (SDH) in the TCA cycle which is important for the electron transport chain by coupling carbon flow to ATP synthesis [35]. The gene encoding ICL has been shown to be up-regulated in persister cells in *B. cenocepacia* biofilms [36]. The authors of this study suggested that surviving persister cells downregulate the TCA cycle to avoid production of ROS and at the same time activate an alternative pathway, the glyoxylate shunt. Employing a combined RNA-Seq and proteomics approach we found that the two ICL genes present in the H111 genome as well as genes/proteins involved in ROS scavenging such as catalases, AhpC and several thioredoxins were up-regulated by low oxygen. Given that the same genes were also up-regulated in micro-oxia in strain J2315 [21], it is tempting to speculate that this pathway is used by *B. cenocepacia* to sustain production of ATP under micro-oxic conditions.

A phenotypical characterization revealed that micro-oxic cells grew better with purines as C-source. The up-regulation of two adenosine deaminases (Table 2 and Table S1) which are key enzymes of purine metabolism and convert adenosine to inosine suggest a role of purine metabolism in micro-oxia. Interestingly, a recent report on hepatocarcinoma-derived cells showed that purines such as inosine and adenosine have a cytoprotective effect and can serve as an alternative source of energy to produce ATP during hypoxic conditions [37]. The ribose moiety of adenosine and purine could be used as a precursor for the phosphorylated glycolytic intermediates in reactions catalyzed by the pentose phosphate (PP) pathway. Among the genes up-regulated in micro-oxia (Table S1) we also found several nucleoside phosphorylases

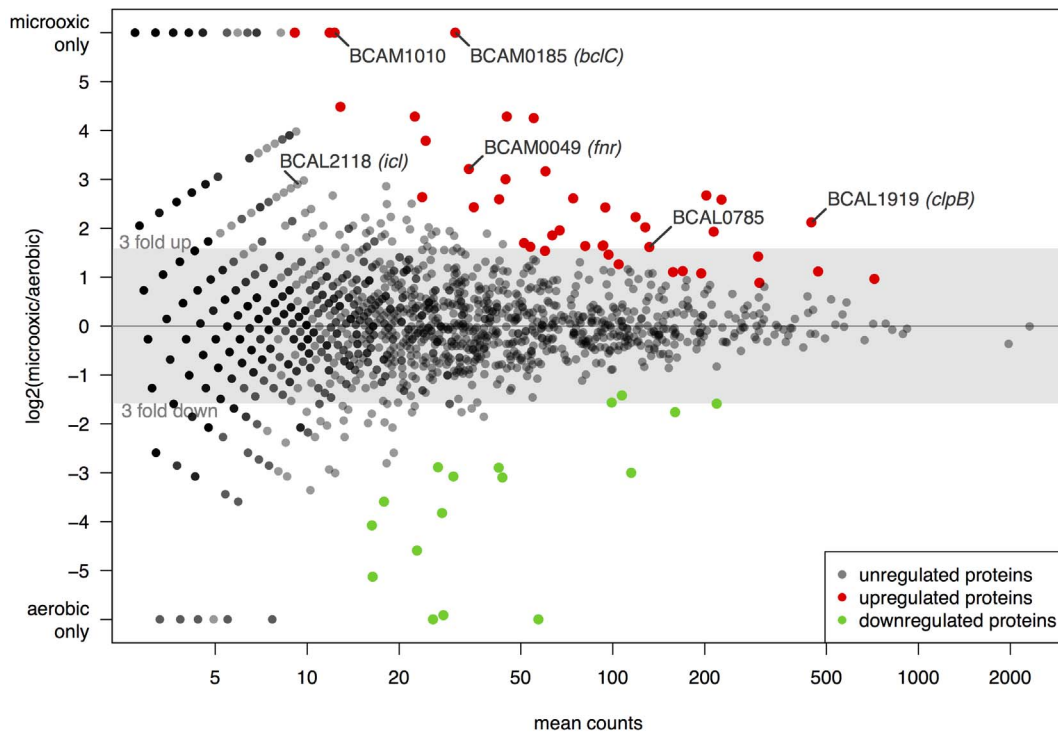


Figure 5. Differential protein expression under micro-oxic and aerobic conditions. MA plot showing the log₂ fold change in protein expression of *B. cenocepacia* H111 grown under micro-oxic versus aerobic conditions. The top regulated proteins are shown in color: proteins with increased expression under micro-oxic conditions are indicated in red, down-regulated proteins in green.
doi:10.1371/journal.pone.0072939.g005

which catalyse the reversible phosphorylation of purine (2'-deoxy)ribonucleosides to free bases and (2'-deoxy)ribose 1-phosphates. This could represent another possibility for *B. cenocepacia* to generate energy under micro-oxic conditions.

In this study we showed that micro-oxic conditions promoted biofilm formation of *B. cenocepacia*. Similar observations have been made for *P. aeruginosa*, which produces more alginate when oxygen is limiting [38–40]. Our global expression analyses revealed the up-regulation of three regions potentially responsible for increased biofilm formation under micro-oxic conditions: i) the EPS cepacian encoding gene cluster *BCAM1004-10* [41,42] ii) the lectin gene *BCAM0185* [43], and iii) the gene encoding the large surface protein BapA, which was previously shown to be important for biofilm formation [43].

The observation that cells growing micro-oxically were more resistant to several antibiotics is probably due to their slower growth rate compared to aerobically growing cells. Muir et al. showed that the higher the growth rate of cells at the time of antibiotic addition, the greater the growth-inhibitory effect [44].

The effect of low-oxygen tension on gene expression was one of the nine conditions tested by Sass and colleagues in *B. cenocepacia* strain J2315 [21]. Although the experimental settings used in their study were very different from ours (i) shift *versus* run out experiment, ii) CampyGen Compact gas generating system *versus* controlled gas atmosphere, iii) 6% *versus* 0.5% oxygen, iv) strain J2315 *versus* H111) and different analysis technologies were used (microarray *versus* RNA-Seq), there was a good overlap between the two data sets. In fact, 55 of the 176 H111 genes/proteins reported here were also differentially expressed in response to low oxygen in strain J2315 (Table S2). Among them are universal stress proteins, the protease ClpB, the isocitrate lyase BCAL2118,

arginine/ornithine decarboxylases, the cytochrome d ubiquinol oxidase and several membrane proteins. In line with the observation that strain H111 produces reduced amounts of siderophores in micro-oxia, several TonB dependent receptors were down-regulated in micro-oxic conditions. The *lxa* locus as well as the cable pilus cluster (*cbh*), which are both induced in strain J2315, are absent in strain H111. Other gene clusters for flagellar and chemotaxis proteins were up-regulated only in strain J2315. Among the genes specifically induced in strain H111 we found the fimbriae encoding gene *fimA* (*BCAL1677*), an adenosine deaminase (*BCAM2458*), several porins (*BCAM2723*, *BCAL3007*, *BCAM2462*) and several ABC transporters. Among the transcriptional regulators highly up-regulated in micro-oxia in both studies was the FNR-type regulator BCAM0049 (Table 2). Orthologous proteins have been shown to sense the oxygen tension and control gene expression under low oxygen conditions in several organisms [28,45]. The *P. aeruginosa* FNR-type regulator ANR is known to positively control expression of denitrification and arginine fermentation genes. This regulator could also play an important role in the regulation of genes in micro-oxic conditions.

In conclusion, we have shown that *B. cenocepacia* H111 can grow with as little as 0.1% oxygen but is not able to grow anaerobically. Since *P. aeruginosa* grows anaerobically and has been shown to occupy deeper sites within wounds [46] it appears likely that *B. cenocepacia* may occupy a different niche where oxygen is limited but not totally absent. Our study provides a list of the most significant differentially expressed genes/proteins in micro-oxically versus aerobically grown cells and opens new avenues in the understanding of the molecular mechanism underlying the physiology and regulation of the *in vivo* relevant micro-oxic lifestyle of *B. cenocepacia*.

Table 2. List of 176 *B. cenocepacia* H111 genes/proteins that showed differential expression in micro-oxic (M) conditions compared to aerobic (A) conditions (DESeq analysis, p-value<0.15 for proteomics and p-value<0.2 for RNA-Seq).

Locus ID ^a	Orthologs J2315 ^b	Description ^a	Tp ^c	Proteome FC(M/A) ^d	RNASeq FC(M/A) ^e
Amino acid transport and metabolism					
CCE49364	BCAL0010	Phenylalanine-4-hydroxylase		3.2	1.4
CCE53410	BCAL0705	D-alanine aminotransferase		-1.2	17.4
CCE52708	BCAL2198	Cysteine desulfurase, IscS subfamily		-7.5	-2.4
CCE50178	BCAL2213	Oligopeptidase A		1.5	11.7
CCE48700	BCAM1111	Ornithine decarboxylase		6.1	2.5
CCE48699	BCAM1112	Arginine decarboxylase/Ornithine decarboxylase		6.0	2.2
CCE47458	BCAM1306	Amino acid permease	TM	nd	16.6
CCE47406	BCAM1353	Alanine dehydrogenase		nd	M only
CCE46974	BCAM1735	Glucose dehydrogenase, membrane-bound, flavoprotein	TM	-60.3	-1.4
CCE53212	BCAM2094	Glutamine synthetase family protein		nd	15.1
CCE47595	BCAM2482	Agmatinase		nd	19.8
CCE51862	BCAS0081	ABC transporter		nd	27.9
CCE52306	BCAS0451	ABC transporter ATP-binding protein		nd	19.4
CCE52596	BCAS0602	Permease of the metabolite transporter (DMT) superfamily	TM	nd	M only
Energy production and conversion					
CCE49315	BCAL0052	D-2-hydroxyglutarate dehydrogenase		nd	15.0
CCE48192	BCAL0522	Flagellum-specific ATP synthase FliI		nd	A only
CCE48177	BCAL0536	Ferredoxin-NAD(+) reductase		3.1	1.4
CCE53334	BCAL0785	Cytochrome d ubiquinol oxidase subunit I	TM	3.1	6.7
CCE50746	BCAL1831	Aldehyde dehydrogenase		3.1	1.3
CCE52795	BCAL2118	Isocitrate lyase		7.5	24.9
CCE49032	BCAL2685	Sulfite reductase [NADPH] hemoprotein β-component		-16.9	-1.5
CCE51244	BCAL3285	Flavo-hemoprotein		nd	51.7
CCE46730	BCAM0175	Malate:quinone oxidoreductase	S	-8.4	-3.6
CCE47517	BCAM1250	Acetyl-CoA hydrolase		9.0	5.5
CCE47209	BCAM1537	Putative oxidoreductase YncB		6.0	9.4
CCE47172	BCAM1570	Alcohol dehydrogenase		4.7	7.6
CCE47153	BCAM1581	Phosphoenolpyruvate carboxykinase [GTP]		8.0	5.6
CCE46975	BCAM1734	Glucose dehydrogenase	S	-7.4	-8.3
CCE53213	BCAM2093	Salicylate hydroxylase		nd	28.5
CCE46457	BCAM2710	Protein acetyltransferase		19.5	1.9
CCE51861	BCAS0080	FAD-dependent NAD(P)-disulphide oxidoreductase		nd	28.1
Nucleotide transport and metabolism					
CCE47622	BCAM2458	Adenosine deaminase		nd	31.2
CCE48624	BCAM0402	Cytidine/deoxycytidylate deaminase family protein		nd	20.8
Carbohydrate transport and metabolism					
CCE51300	BCAL3342	Phosphoglycerate mutase		1.8	-19.1
CCE46772	BCAM0154	4-deoxy-L-threo-5-hexosulose-uronate ketol-isomerase		nd	16.9
Coenzyme transport and metabolism					
CCE49767	BCAL2975	Periplasmic molybdate-binding domain protein		nd	17.3
CCE49194	BCAM0010	2-amino-3-ketobutyrate coenzyme A ligase		2.9	1.7
Lipid transport and metabolism					
CCE49544	BCAL1863	Polyhydroxyalkanoic acid synthase		6.2	1.4
CCE48735	BCAM1005	O-antigen acetylase	TM	nd	M only
CCE53016	BCAM2232	2,3-dihydroxybenzoate-AMP ligase siderophore		nd	-38.2
Translation, ribosomal structure and biogenesis					

Table 2. Cont.

Locus ID ^a	Orthologs J2315 ^b	Description ^a	Tp ^c	Proteome FC(M/A) ^d	RNASeq FC(M/A) ^e
CCE49086	BCAL0231	Translation elongation factor G		1.4	9.9
Transcription					
CCE49231	BCAL0124	Flagellar transcriptional activator FlhD		nd	-19.1
CCE48084	BCAL0625	Transcriptional regulator		M only	1.6
CCE51487	BCAL1210	Transcriptional regulators, LysR family		nd	14.8
CCE46853	BCAM0049	Transcriptional regulator, CRP family		9.3	3.8
CCE46759	BCAM0167	Transcriptional regulator, LysR family		nd	21.4
CCE48623	BCAM0403	Acetyltransferase		nd	22.9
CCE48936	BCAM0751	Transcriptional regulator, LysR family		nd	11.7
CCE47511	BCAM1257	Transcriptional regulator, MerR family		nd	M only
CCE47508	BCAM1259	RpoD-related RND polymerase sigma factor		nd	26.4
CCE47210	BCAM1536	Transcriptional regulator, TetR family		1.7	20.7
CCE52597	BCAS0603	Transcriptional regulator, AraC family		nd	28.1
CCE53209		Transcriptional regulator, TetR family		nd	14.6
Replication, recombination and repair					
CCE52866	BCAL2278	Transposase		nd	9.7
CCE47509	BCAM1258	Putative DNA polymerase family X		nd	18.5
Cell wall/membrane/envelope biogenesis					
CCE50995	BCAL0940	Membrane carboxypeptidase (penicillin-binding protein)	TM	nd	11.0
CCE51437	BCAL1258	Membrane-bound murein transglycosylase D precursor		-35.0	1.5
CCE47918	BCAL1493	Putative transmembrane protein		-3	-1.5
CCE50748	BCAL1829	Outer membrane protein W precursor	S	6.4	3.8
CCE50709	BCAL2645	Outer membrane protein	TM	3.1	-1.2
CCE49628	BCAL2783	Cyclopropane-fatty-acyl-phospholipid synthase		5.4	3.6
CCE49806	BCAL3008	Outer membrane protein (porin)	S	2.1	2.1
CCE51186	BCAL3204	Peptidoglycan-associated lipoprotein precursor	S	-2.7	-1.3
CCE48736	BCAM1004	GDP-mannose 4,6 dehydratase		M only	12.2
CCE48728	BCAM1010	UTP-glucose-1-phosphate uridylyltransferase		M only	2.7
CCE47356	BCAM1398	Outer membrane protein (porin)	S	-3.4	-4.1
CCE46444	BCAM2723	Outer membrane porin, OprD family	S	nd	20.1
Cell motility					
CCE51168	BCAL0142	Flagellar biosynthesis protein FlhF		4.4	-44.9
CCE48144	BCAL0567	Flagellar hook protein FlgE		-2.2	-10.8
CCE48143	BCAL0568	Flagellar basal-body rod protein FlgF		nd	-20.2
CCE48141	BCAL0570	Flagellar L-ring protein FlgH	S	-2.1	-20.8
CCE48139	BCAL0572	Flagellar protein FlgJ [peptidoglycan hydrolase]		nd	-24.7
CCE47986	BCAL3503	Flagellar biosynthesis protein FlpP	TM	nd	-19.5
CCE47983	BCAL3506	Flagellar motor switch protein FliM		-1.4	-20.7
CCE53442	BCAL1677	Type 1 fimbriae major subunit FimA	S	1.8	M only
Posttranslational modification, protein turnover, chaperones					
CCE48216	BCAL0500	ATP-dependent hsl protease ATP-binding subunit HslU		1.3	13.3
CCE51547	BCAL1070	Alkyl hydroperoxide reductase subunit C-like protein	S	1.0	15.0
CCE51462	BCAL1233	Molecular chaperone (small heat shock protein)		2.1	32.5
CCE51461	BCAL1234	Molecular chaperone (small heat shock protein)		5.3	37.4
CCE49486	BCAL1919	ClpB protein		4.3	20.9
CCE49077	BCAL2730	ATP-dependent protease ATP-binding subunit ClpA		3.9	7.2
CCE49078	BCAL2731	ATP-dependent Clp protease adaptor protein ClpS		2.5	11.0

Table 2. Cont.

Locus ID ^a	Orthologs J2315 ^b	Description ^a	Tp ^c	Proteome FC(M/A) ^d	RNASeq FC(M/A) ^e
CCE49625	BCAL2780	Thioredoxin domain-containing protein EC-YbbN		1.7	10.6
CCE52629	BCAL3146	Heat shock protein 60 family chaperone GroEL		2.7	6.7
CCE51225	BCAL3269	Chaperone protein DnaJ		1.7	12.2
CCE51226	BCAL3270	Chaperone protein DnaK		2.0	8.9
CCE51227	BCAL3271	Thiol-disulfide isomerase and thioredoxins		nd	14.3
CCE51228	BCAL3272	Heat shock protein GrpE		1.1	9.7
CCE47165	BCAM0309	Cell division protein FtsH	TM	nd	17.5
CCE48963	BCAM0727	Membrane protease subunits, stomatin/prohibitin homologs		nd	68.6
CCE46962	BCAM1744	Extracellular protease precursor	S	1.3	-18.2
CCE52630	BCAS0638	Heat shock protein 60 family co-chaperone GroES		2.2	27.6
CCE52633	BCAS0641	serine protease		nd	56.1
Inorganic ion transport and metabolism					
CCE49312	BCAL0055	Copper-translocating P-type ATPase	TM	1.5	11.5
CCE52829	BCAL0447	Ferric iron ABC transporter, permease protein	TM	nd	M only
CCE51464	BCAL1231	Integral membrane protein TerC	TM	nd	M only
CCE49029	BCAL2682	Sulfate adenylyltransferase subunit 2		-14.2	-2.5
CCE51255	BCAL3299	Catalase/Peroxidase		2.4	1.9
CCE48540	BCAM0491	Outer membrane vitamin B12 receptor BtuB	S	-24.1	-2.1
CCE48794	BCAM0948	Outer membrane protein NosA precursor		-8.0	-14.2
CCE47584	BCAM1187	Ferrichrome-iron receptor		A only	-10.9
CCE47171	BCAM1571	Zinc-regulated outer membrane receptor		M only	37.1
CCE49127	BCAM2007	Ferrichrome-iron receptor	S	A only	-13.8
CCE53024	BCAM2224	Outer membrane receptor for ferric-pyochelin FptA	S	nd	-20.2
CCE47643	BCAM2439	Ferrichrome-iron receptor	S	-3.0	-7.3
CCE52627	BCAS0635	Manganese catalase		nd	M only
Secondary metabolites biosynthesis, transport and catabolism					
CCE53019	BCAM2230	Dihydroaeruginoate synthetase PchE		nd	-14.3
CCE53020		Pyochelin synthetase PchF		nd	-27.3
Signal transduction mechanisms					
CCE53457	BCAL1663	Serine protein kinase (PrkA protein)		19.5	16.5
CCE52508	BCAM0276	Universal stress protein UspA		4.1	14.1
CCE50874	BCAM0877	Diadenosine tetraphosphatase		nd	M only
CCE46268	BCAM2563	Aerotaxis sensor receptor protein	TM	nd	10.3
Intracellular trafficking, secretion, and vesicular transport					
CCE47881	BCAL1529	Type II/IV secretion system ATPase TadZ		22.4	1.5
CCE53120	BCAM2140	HlyD family secretion protein	TM	nd	30.7
Others					
CCE49314	BCAL0053	Transcriptional regulator, PadR family		1.1	12.3
CCE51109	BCAL0213	Phenylacetate-CoA oxygenase, PaaJ subunit		nd	-34.8
CCE51108	BCAL0214	Phenylacetate-CoA oxygenase, PaaL subunit		2.9	-10.4
CCE46576	BCAL0342	Uncharacterized protein ImpC		2.2	-1.8
CCE46575	BCAL0343	Uncharacterized protein ImpD		2.2	-1.0
CCE48020	BCAL0683	Hypothetical protein I35_1851		nd	20.6
CCE53333	BCAL0786	Hypothetical protein I35_7268	TM	nd	10.0
CCE51079	BCAL0860	Staphylolytic protease preproenzyme LasA		nd	14.3
CCE50996	BCAL0939	Gfa-like protein		nd	12.2
CCE51463	BCAL1232	Hypothetical protein I35_5360		nd	M only

Table 2. Cont.

Locus ID ^a	Orthologs J2315 ^b	Description ^a	Tp ^c	Proteome FC(M/A) ^d	RNASeq FC(M/A) ^e
CCE51401	BCAL1294	VgrG protein		13.8	2.6
CCE51631	BCAL1463	Ribonuclease BN	TM	nd	21.7
CCE53456	BCAL1664	Hypothetical protein I35_7395		nd	16.7
CCE53455	BCAL1665	SpoVR-like protein		nd	16.4
CCE50747	BCAL1830	Dioxygenase, 2-nitropropane dioxygenase-like		19.1	1.8
CCE50719	BCAL1857	Hypothetical protein I35_4602	TM	nd	16.0
CCE52700	BCAL2206	Granule-associated protein		3.1	9.5
CCE50568	BCAL2439	Hypothetical protein I35_4448	TM	nd	12.9
CCE49604	BCAL2760	UPF0434 protein YcaR		-3.0	A only
CCE49988	BCAL3178	Transcriptional regulator		2.8	1.7
CCE51204	BCAL3243	Capsular polysaccharide biosynthesis/export protein		-8.6	2.2
CCE46874	BCAM0028	Hypothetical protein I35_0684		nd	31.2
CCE46761	BCAM0165	Hypothetical protein I35_0571		nd	-14.1
CCE46721	BCAM0185	Lectin BcIC		M only	7.1
CCE48935	BCAM0752	Hydrolase-related protein		nd	15.2
CCE47460	BCAM1304	Phage-related protein		nd	10.6
CCE47459	BCAM1305	hypothetical protein I35_1271		nd	10.8
CCE47408	BCAM1351	DnaK suppressor protein		nd	16.2
CCE47407	BCAM1352	DNA-dependent DNA polymerase family X		nd	27.2
CCE47250	BCAM1500	Universal stress protein family		5.4	5.6
CCE47213	BCAM1534	Chromosome segregation ATPases		nd	43.6
CCE47212	BCAM1535	Hypothetical protein I35_1024	S	nd	18.0
CCE47173	BCAM1569	Neuraminidase (sialidase)	S	nd	13.9
CCE50317	BCAM1926	CBS domain protein		1.2	10.2
CCE53123	BCAM2137	Transcriptional regulatory protein		nd	20.0
CCE53121	BCAM2139	Eukaryotic putative RNA-binding region RNP-1 signature		nd	M only
CCE53091	BCAM2167	Hypothetical protein I35_7022		nd	15.6
CCE53041	BCAM2210	Hypothetical protein I35_6972	TM	nd	M only
CCE47618	BCAM2462	Outer membrane protein (porin)	S	nd	55.2
CCE47617	BCAM2463	Hypothetical protein I35_1430		nd	10.2
CCE51782	BCAS0002	Chromosome (plasmid) partitioning protein ParB		1.3	19.1
CCE51864	BCAS0082	Hydrolases of the alpha/beta superfamily	TM	nd	21.1
CCE52109	BCAS0293	AidA		2.2	M only
CCE52595	BCAS0601	Putative ATP/GTP-binding protein		nd	28.5
CCE52677	BCAS0723	Putative cytoplasmic protein		nd	30.7
CCE46207		Outer membrane protein (porin)	S	2.2	2.0
CCE46671		Hypothetical protein I35_0480		nd	-9.6
CCE47170		Hypothetical protein I35_0982		nd	52.5
CCE47794		Hypothetical protein I35_1612		nd	M only
CCE48729		Hypothetical protein I35_2566	TM	nd	M only
CCE50639		Shufflon-specific DND recombinase		nd	10.6
CCE51201		Capsular polysaccharide export system protein KpsE	TM	-12.1	1.2
CCE52058		Quinone oxidoreductase (NADPH:quinone reductase)		nd	14.0
CCE52231		Histone acetyltransferase HPA2		nd	M only
CCE52465		29 kDa antigen		3.6	-2.3
CCE52505		Regulator of competence-specific genes		M only	15.4
CCE52619		TPR repeat protein, SEL1 subfamily	S	nd	17.1

Table 2. Cont.

Locus ID ^a	Orthologs J2315 ^b	Description ^a	Tp ^c	Proteome FC(M/A) ^d	RNASeq FC(M/A) ^e
CCE52635		Hypothetical protein I35_6546		nd	16.3
CCE52659		Tannase precursor		nd	24.9
CCE52669		Hypothetical protein I35_6580		nd	23.4
CCE53181		Cyclohexanone monooxygenase		nd	31.2
CCE53450		Large exoproteins involved in heme utilization		3.8	1.9

^aNomenclature and description according to GenBank file CAFQ01000001.1.

^bOrthologs were identified as described in the Material and Methods section.

^cPredicted topology (Tp) according to SignalP v4.0 (secreted proteins, S) and TMHMM v2.0 (transmembrane, TM).

^dFold change (FC) of protein expression, comparing micro-oxically (M) with aerobically (A) grown wild-type strain.

^eFold change (FC) of transcript expression, comparing micro-oxically (M) with aerobically (A) grown wild-type strain.

nd: The gene was not identified on protein level.

M only and A only: The gene/protein was detected only micro-oxically (M) or aerobically (A).

The proNOG categories are indicated and the 58 differentially expressed proteins are indicated in bold. The overlap in low oxygen regulation with strain J2315 (Sass et al., 2013) is indicated in italics.

doi:10.1371/journal.pone.0072939.t002

Materials and Methods

Bacterial strains, plasmids and growth conditions

B. cenocepacia wild type H111 [22,47,48] was grown under aerobic (21% oxygen) and micro-oxic conditions (0.1% to 5% oxygen) at 37°C in LB Lennox broth (Difco) or ABC Minimal Medium containing citrate as carbon source [49]. Aerobic cultures were grown with rigorous shaking (220 rpm) in 500-mL Erlenmeyer flasks containing 25 ml medium or, for RNA-Seq and proteomics experiments, in 1-L Erlenmeyer flasks containing 100 ml medium. Micro-oxic liquid cultures were grown under a nitrogen gas atmosphere that contained 5% or 0.5% or 0.1% oxygen with moderate shaking (80 rpm) in 500-ml rubber-stoppered serum bottles containing 50 ml medium. The gas phase (e. g. 0.5% O₂, 99.5% N₂) was exchanged every 8–14 hours. For the cultivation of bacteria on plates, micro-oxic conditions were created using the CampyGen Compact gas generating system (oxid) by quickly changing the paper sachet every 24 hours and keeping the exposure to atmospheric oxygen at a minimum.

Phenotypical analysis

Biofilm formation was quantified in a microtiter dish assay as described by Huber *et al.* [50]. Since micro-oxic and aerobic cells reached different optical densities (OD), we used the biofilm index (BI) to compare the amounts of biofilm formed. The BI was calculated as the mean percentage ratio between OD₅₇₀ after crystal violet staining and OD₅₅₀ measured before incubating the cells with crystal violet which reflects the total cell number [51]. The formation of pellicles was assessed in NYG medium (0.5% peptone, 0.3% yeast extract, 2% glycerol) according to Fazli *et al.*, 2011 [52]. Proteolytic activity was quantified based on the method described by Schmid *et al.* [53] growing cells in NYG medium at 37°C to late exponential growth phase and using azocasein (5 mg/ml, in 50 mM Tris-Cl pH 8) for 60 min at 37°C as substrate. For quantification of lipases and cellulases, the sterile culture supernatant was incubated with buffer 1 (1 volume 0.3% p-nitrophenyl palmitate in isopropanol and 9 volumes of 0.2% sodiumdesoxycholate and 0.1% gum arabicum in 50 mM sodiumphosphate buffer pH 8) and 1% carboxymethylcellulose, respectively. After incubation, the absorbance was measured at 410 nm and 575 nm, respectively [50]. A Bradford assay (Coomassie PlusTM, Thermo Scientific/Pierce) with BSA as standard was used to determine the total protein concentration

in extracts derived from both aerobic and micro-oxic cultures. Antibiotic susceptibility testing was performed on agar plates where bacteria were homogeneously spread over the surface of the agar plate. Antibiotic discs (kanamycin 30 µg, tetracycline 30 µg, gentamycin 10 µg; Alere GmbH) were placed in the center of the plate. Swarming and swimming were tested by inoculating cells onto plates containing ABC medium supplemented with 0.1% casamino acids that were solidified with 0.4% and 0.3% agar, respectively. Plates were incubated for 2 days. Siderophores production was measured on CAS plates as described previously [54]. All phenotypic assays were performed at least in triplicate.

Biolog analysis

B. cenocepacia was streaked on R2A agar plates and grown overnight at 37°C. From this plate, colonies were picked up and suspended in the GN/GP-IF at the required optical density. The suspensions were then inoculated on Biolog plates PM1 and PM2a for the carbon sources and PM3b for the nitrogen sources (Biolog, Hayward, CA). Plates were incubated at 37°C for 24 h fully aerated or for 36 h under micro-oxic conditions using CampyGen jars (Oxoid, Basingstoke, UK). The optical density was measured using a plate reader; instances where a >50% OD₆₀₀ difference was observed between micro-oxic and aerobic cells were deemed significant [55]. Each condition was tested in triplicate.

RNA-Seq and data analysis

Total RNA from *B. cenocepacia* strain H111 grown with 21% or 0.5% oxygen in complex LB medium to the end of the exponential phase (OD₆₀₀ of 0.8 and 0.4, respectively, Figure 1) was extracted using a modified hot acid phenol protocol [56]. The removal of genomic DNA using DNaseI (Promega) was verified by a PCR reaction with 40 cycles. The samples were then further purified using the RNeasy kit (Qiagen) and the RNA quality was checked using RNA Nano Chips (Agilent 2100 Bioanalyzer; RIN >8). The RNA samples were poly(A)-tailed using poly(A) polymerase. Then, the 5'PPP were removed using tobacco acid pyrophosphatase (TAP). Afterwards, an RNA adapter was ligated to the 5'-monophosphate of the RNA. First-strand cDNA synthesis was performed using an oligo(dT)-adapter primer and the M-MLV reverse transcriptase (Promega). The resulting cDNA was PCR-amplified to about 20–30 ng/µl using a high fidelity DNA polymerase. The cDNA was purified using the Agencourt AMPure

XP kit (Beckman Coulter Genomics) and was analyzed by capillary electrophoresis. The primers used for PCR amplification were designed for TruSeq sequencing according to the instructions of Illumina. Illumina single-end sequencing was performed on a HiSeq2000 instrument. The sequence reads were processed and then mapped to the *B. cenocepacia* H111 genome using CLC Genomics Workbench v4.9 (CLC bio) allowing up to 2 mismatches per read. The mapped reads (or spectral counts, see below) were analyzed using the DESeq software [30]. DESeq models gene/protein expression with a negative binomial distribution and outputs a list of differentially expressed genes/proteins ranked according to statistical significance. We report the top 123 differentially expressed genes (p-value cut-off <0.2), i.e. approx. 2.5% of the genes found actively expressed. This model is more robust against over-identifying candidate regulated genes based on fold-change alone, which can in particular be problematic for genes that are identified with few sequencing reads (common for *Burkholderia* with their high GC content, [57]) or spectra. We only considered genes with five or more reads for differential analysis. For functional annotation of H111 genes, we relied on the eggNOG resource [31] and transferred the functional annotations from the respective J2315 orthologs as described [53]. The RNA-Seq raw data files are accessible through the GEO Series accession number GSE48585.

Preparation of protein samples

Extracellular proteins and subcellular fractions were prepared as described previously [53]. Cells were lysed by two consecutive passes through a French Press homogenizer (Hypramag/Aminco), and cell debris was removed by 15 min centrifugation at 4000 g. Total cell membranes were subsequently harvested by ultracentrifugation for 1 h at 80000 g, 4°C. The pellet containing total membrane proteins was dissolved in 100 mM Tris-HCl, pH 7.5, 2% SDS by incubation at 50°C for 1 h. The cell lysate supernatant containing soluble cytoplasmic proteins was extracted with 6 volumes of ice-cold acetone at -20°C overnight. The precipitated proteins were harvested by centrifugation at 20000 g and dissolved in 100 mM Tris-HCl, pH 7.5, 0.1% SDS. Total protein concentration was determined according to Bradford (Coomassie Plus™ protein assay, Pierce). Approximately 15 mg total protein for each extracellular (EC), cytoplasmic (Cyt) and total membrane (TM) fractions were separated by 1D SDS-PAGE on 12.5% polyacrylamide gels. Gels were stained with colloidal Coomassie Blue (Serva). Individual protein lanes were cut into ten slices and immediately subjected to in-gel tryptic digestion [58].

Mass spectrometry, protein identification and differential expression analysis

Peptides were separated by RP-HPLC and analyzed by a hybrid LTQ-Orbitrap XL mass spectrometer (Thermo Fisher Scientific, Waltham, MA, USA) interfaced with a nano-electrospray source. Mass spectrometric detection was performed in data-dependent mode. Precursor mass spectra were acquired at the Orbitrap mass analyzer with a scan range from m/z 300 to 1,600; resolution was set to 60,000 at m/z 400. Mass spectra were processed with Xcalibur 2.0.7 (Thermo Fisher Scientific) and peak lists were generated with msConvert (version 3.0.4388) [59]. Fragment ion mass spectra were searched with MS-GF+ (MS-GFDB v7747) against a sequence database consisting of 7,258 *B. cenocepacia* strain H111 proteins (accession CAFQ00000000.1) and 259 common contaminants (e.g. human keratin, trypsin). Spectra were searched for a match to fully-tryptic and semi-tryptic peptides with a mass tolerance of 10ppm. Carbamidomethylation was set as fixed modification for all cysteines while oxidation of methionines,

deamidation of asparagines and glutamines as well as cyclization of N-terminal glutamines were considered as optional modifications.

Based on the target-decoy search strategy [60], a stringent score cutoff was determined that resulted in an estimated FDR of less than 0.2% at the PSM level. PSMs above this cutoff were subjected to a PeptideClassifier analysis [61] and only peptides that unambiguously identify one protein (either class 1a or 3a) were considered. We furthermore required at least 3 independent spectra or two spectra from two distinct peptides for protein identification. Each subcellular fraction was measured once with a discovery run followed by a subsequent exclusion list run (precursor ions identified in the discovery run were excluded from fragmentation in the exclusion run) [29]. Thereby, about 15% more proteins (272), all preferentially lower abundant, could be added by the exclusion list approach to those identified over all respective first runs (1854, Figure S3). This resulted in a total of 2128 identified proteins at an estimated FDR of less than 1% (0.98%). Total spectral counts for each protein were used for a differential expression analysis with the R package DESeq (version 1.6.1, [30]). Due to the lower number of spectral counts compared to sequenced reads, we chose a more lenient cut-off of p<0.15 to select the 58 top-ranked differentially expressed proteins for further analysis (roughly 2.7% of all proteins expressed). Protein abundance was estimated according to the method of Schrimpf et al. [62] (Figure S3). Proteomics data associated with this manuscript can be downloaded from the ProteomeXchange under accession number PXD000270. Signal peptide predictions from SignalP (version 4.0), and transmembrane domain predictions from TMHMM (version 2.0; both from the CBS, Denmark), were used for a combined topology prediction: Proteins without a predicted transmembrane domain after a predicted signal peptide cleavage site are considered secreted. Proteins with one or more predicted transmembrane domains after a predicted signal peptide cleavage site or without a predicted signal peptide cleavage site are assumed to be transmembrane proteins.

Construction and assessment of transcriptional *lacZ* fusions

For construction of transcriptional *lacZ* fusions, vector pSU11p [53] was used. The promoter regions of *BCAL2780*, *BCAM1259*, *wcaJ* genes were first amplified using the primers listed in Table S4 and cloned into vector pCR 2.1 TOPO (Invitrogen, Carlsbad, CA). After sequence verification, the promoter probes were cut and cloned into pSU11p using HindIII and XhoI. The resulting plasmids pP_{BCAL2780}-*lacZ*, pP_{BCAM1259}-*lacZ* and pP_{wcaJ}-*lacZ* were transferred by triparental mating into *B. cenocepacia* strain H111 and β-galactosidase activity was determined both under micro-oxic and aerobic conditions by the Miller method [63]. Briefly, the strains were grown overnight in LB broth, then subcultured in LB medium and incubated for 2 days (aerobic cultures) or 4 days (micro-oxic cultures). The experiment was run in triplicate. β-galactosidase activity was also visually inspected on LB plates containing 5-bromo-4-chloro-3-indolyl-β-D-galactoside (X-Gal) (Sigma). Bacterial strains, plasmid and primers used in this study are listed in Table S4.

qPCR analyses

The expression of H111 orthologs of J2315 genes *BCAM1259*, *BCAL0785*, *BCAL1919*, *BCAM1010*, *BCAM0049* and *BCAL2118* was analyzed with a Mx3000P instrument using Brilliant III Ultra-Fast SYBR® Green QPCR Master Mix (Agilent, Switzerland) and cDNA prepared from biological replicates as template. Each reaction contained 12.5 μl 2× Brilliant III Ultra-Fast SYBR® Green QPCR Master Mix, 0.7 μM of individual primers and 15

or 7.5 or 3.5 ng of cDNA in a total volume of 25 μ l. Reactions were run in triplicates. The relative expression ratio was calculated according to Pfaffl [64] using the primary sigma factor *rhoD* (*BCAM0918*) as housekeeping gene. The primers used are listed in Table S4.

Statistical analyses

Continuous normally distributed data were analyzed by using an independent sample t-test. P-values were determined using SPSS software, version 21.0. The over-representation analysis of EggNOG functional categories was carried out using Fisher's Exact tests.

Supporting Information

Figure S1 Decreased siderophore production in micro-oxic conditions. Siderophore production of *B. cenocepacia* H111 grown under aerobic (black bar) and micro-oxic (grey bar) conditions was measured on CAS plates. The measured halo diameter corresponds to siderophore activity. Whiskers indicate SD, n = 3. (TIF)

Figure S2 Validation of four micro-oxic induced genes by *lacZ* fusions. The activity of BCAL2780 (thioredoxin domain containing protein), BCAM1259 (sigma factor), *wcaJ* (CCE50896, sugar transferase in cepacian cluster II), *bclA* (lectin) and *cepI* promoter fusion was determined in the wild type grown in aerobic (black bar) and micro-oxic (grey bar) conditions. Whiskers indicate SD, n = 3. (TIF)

Figure S3 Proteins identified by the exclusion list approach add 272 preferentially low abundant proteins. The exclusion list approach was successful in adding preferentially lower abundant proteins (red curve) on top of those identified over

all discovery runs (blue curve) and allowed us to dig deeper into the proteome. For calculation of the relative protein abundance, see Methods.

(TIF)

Table S1 Shotgun proteomics and RNA-Seq data for all *B. cenocepacia* H111 genes/proteins grown in micro-oxic (M) conditions and aerobic (A) conditions.

(XLSX)

Table S2 List of 55 *B. cenocepacia* H111 and J2315 genes that are commonly induced by low oxygen (M) (DESeq analysis, p-value < 0.2 for H111, fold change > 2 for J2315). The expression in aerobic cells was taken as baseline (A).

(XLSX)

Table S3 Q-PCR results for selected genes.

(XLSX)

Table S4 Bacterial strains, plasmids and oligonucleotides used in this study.

(DOCX)

Acknowledgments

We gratefully acknowledge Cynthia Sharma and Konrad Förstner (University of Würzburg) for processing our RNA-Seq samples. We thank Martina Lardi for help in statistical analysis and Kirsty Agnoli for assistance in processing Biolog plates. Hans-Martin Fischer is acknowledged for providing access to the gas station at the Microbiology Institute of the ETH Zurich.

Author Contributions

Conceived and designed the experiments: GP CHA LE. Performed the experiments: GP RB AG. Analyzed the data: GP RB AG UO CHA LE. Wrote the paper: GP LE.

References

- Mahenthalingam E, Urban TA, Goldberg JB (2005) The multifarious, multireplicon *Burkholderia cepacia* complex. Nat Rev Microbiol 3: 144–156.
- Mahenthalingam E, Baldwin A, Dowson CG (2008) *Burkholderia cepacia* complex bacteria: opportunistic pathogens with important natural biology. J Appl Microbiol 104: 1539–1551.
- Burns JL (2007) Antibiotic resistance of *Burkholderia* spp.; H. B, editor. Norfolk: New Horizon.
- LiPuma JJ, Dasen SE, Nielson DW, Stern RC, Stull TL (1990) Person-to-person transmission of *Pseudomonas cepacia* between patients with cystic fibrosis. Lancet 336: 1094–1096.
- Drevinek P, Mahenthalingam E (2010) *Burkholderia cenocepacia* in cystic fibrosis: epidemiology and molecular mechanisms of virulence. Clin Microbiol Infect 16: 821–830.
- Döring G, Parameswaran IG, Murphy TF (2011) Differential adaptation of microbial pathogens to airways of patients with cystic fibrosis and chronic obstructive pulmonary disease. FEMS Microbiol Rev 35: 124–146.
- Worlitzsch D, Tarran R, Ulrich M, Schwab U, Cekici A, et al. (2002) Effects of reduced mucus oxygen concentration in airway *Pseudomonas* infections of cystic fibrosis patients. J Clin Invest 109: 317–325.
- Yoon SS, Hennigan RF, Hilliard GM, Ochsner UA, Parvatiyar K, et al. (2002) *Pseudomonas aeruginosa* anaerobic respiration in biofilms: relationships to cystic fibrosis pathogenesis. Dev Cell 3: 593–603.
- Hassett DJ, Cuppoletti J, Trapnell B, Lymar SV, Rowe JJ, et al. (2002) Anaerobic metabolism and quorum sensing by *Pseudomonas aeruginosa* biofilms in chronically infected cystic fibrosis airways: rethinking antibiotic treatment strategies and drug targets. Adv Drug Deliv Rev 54: 1425–1443.
- Xu KD, Stewart PS, Xia F, Huang CT, McFeters GA (1998) Spatial physiological heterogeneity in *Pseudomonas aeruginosa* biofilm is determined by oxygen availability. Appl Environ Microbiol 64: 4035–4039.
- Tunney MM, Field TR, Moriarty TF, Patrick S, Döring G, et al. (2008) Detection of anaerobic bacteria in high numbers in sputum from patients with cystic fibrosis. Am J Respir Crit Care Med 177: 995–1001.
- Alvarez-Ortega C, Harwood CS (2007) Responses of *Pseudomonas aeruginosa* to low oxygen indicate that growth in the cystic fibrosis lung is by aerobic respiration. Mol Microbiol 65: 153–165.
- Sabra W, Kim EJ, Zeng AP (2002) Physiological responses of *Pseudomonas aeruginosa* PAO1 to oxidative stress in controlled microaerobic and aerobic cultures. Microbiology 148: 3195–3202.
- Zumft WG (1997) Cell biology and molecular basis of denitrification. Microbiol Mol Biol Rev 61: 533–616.
- Yang L, Jelsbak L, Molin S (2011) Microbial ecology and adaptation in cystic fibrosis airways. Environ Microbiol 13: 1682–1689.
- Schober M, Jahn D (2010) Anaerobic physiology of *Pseudomonas aeruginosa* in the cystic fibrosis lung. Int J Med Microbiol 300: 549–556.
- Arai H (2011) Regulation and function of versatile aerobic and anaerobic respiratory metabolism in *Pseudomonas aeruginosa*. Front Microbiol 2: article 103.
- Vander Wauwen C, Pierard A, Kley-Raymann M, Haas D (1984) *Pseudomonas aeruginosa* mutants affected in anaerobic growth on arginine: evidence for a four-gene cluster encoding the arginine deiminase pathway. J Bacteriol 160: 928–934.
- Eschbach M, Schreiber K, Trunk K, Buer J, Jahn D, et al. (2004) Long-term anaerobic survival of the opportunistic pathogen *Pseudomonas aeruginosa* via pyruvate fermentation. J Bacteriol 186: 4596–4604.
- Lieberman TD, Michel JB, Aingaran M, Potter-Bynoe G, Roux D, et al. (2011) Parallel bacterial evolution within multiple patients identifies candidate pathogenicity genes. Nat Genet 43: 1275–1280.
- Sass AM, Schmerk C, Agnoli K, Norville PJ, Eberl L, et al. (2013) The unexpected discovery of a novel low-oxygen-activated locus for the anoxic persistence of *Burkholderia cenocepacia*. ISME J; doi: 10.1038/ismej.2013.1036.
- Geisenberger O, Givskov M, Riedel K, Hoiby N, Tümmler B, et al. (2000) Production of *N*-acetyl-L-homoserine lactones by *P. aeruginosa* isolates from chronic lung infections associated with cystic fibrosis. FEMS Microbiol Lett 184: 273–278.
- Wongwanich S, Chotanachan P, Kondo E, Kanai K (1996) Multifactorial pathogenic mechanisms of *Burkholderia pseudomallei* as suggested from comparison with *Burkholderia cepacia*. Southeast Asian J Trop Med Public Health 27: 111–118.
- Tandhavanant S, Thanwisai A, Limmathurotsakul D, Korbsrisate S, Day NP, et al. (2010) Effect of colony morphology variation of *Burkholderia pseudomallei* on intracellular survival and resistance to antimicrobial environments in human macrophages *in vitro*. BMC Microbiol 10: 303.

25. Pitcher RS, Brittain T, Watmough NJ (2002) Cytochrome cbb(3) oxidase and bacterial microaerobic metabolism. *Biochem Soc Trans* 30: 653–638.
26. Cosseau C, Batut J (2004) Genomics of the *ccaNOQP*-encoded cbb3 oxidase complex in bacteria. *Arch Microbiol* 181: 89–96.
27. Comolli JC, Donohue TJ (2004) Differences in two *Pseudomonas aeruginosa* cbb3 cytochrome oxidases. *Mol Microbiol* 51: 1193–1203.
28. Galimand M, Gamper M, Zimmermann A, Haas D (1991) Positive FNR-like control of anaerobic arginine degradation and nitrate respiration in *Pseudomonas aeruginosa*. *J Bacteriol* 173: 1598–1606.
29. Kristensen DB, Brond JC, Nielsen PA, Andersen JR, Sorensen OT, et al. (2004) Experimental Peptide Identification Repository (EPIR): an integrated peptide-centric platform for validation and mining of tandem mass spectrometry data. *Mol Cell Proteomics* 3: 1023–1038.
30. Anders S, Huber W (2010) Differential expression analysis for sequence count data. *Genome Biol* 11: R106.
31. Powell S, Szklarczyk D, Trachana K, Roth A, Kuhn M, et al. (2012) eggNOG v3.0: orthologous groups covering 1133 organisms at 41 different taxonomic ranges. *Nucleic Acids Res* 40: D284–289.
32. Stewart PS, Franklin MJ (2008) Physiological heterogeneity in biofilms. *Nat Rev Microbiol* 6: 199–210.
33. Pett-Ridge J, Firestone MK (2005) Redox fluctuation structures microbial communities in a wet tropical soil. *Appl Environ Microbiol* 71: 6998–7007.
34. Watanabe S, Zimmermann M, Goodwin MB, Sauer U, Barry CE, . (2011) Fumarate reductase activity maintains an energized membrane in anaerobic *Mycobacterium tuberculosis*. *PLoS Pathog* 7: e1002287.
35. Eoh H, Rhee KY (2013) Multifunctional essentiality of succinate metabolism in adaptation to hypoxia in *Mycobacterium tuberculosis*. *Proc Natl Acad Sci U S A* 110: 6554–6559.
36. Van Acker H, Sass A, Bazzini S, De Roy K, Udine C, et al. (2013) Biofilm-grown *Burkholderia cepacia* complex cells survive antibiotic treatment by avoiding production of reactive oxygen species. *PLoS One* 8: e58943.
37. Modis K, Gero D, Stangl R, Rosero O, Szijarto A, et al. (2013) Adenosine and inosine exert cytoprotective effects in an *in vitro* model of liver ischemia-reperfusion injury. *Int J Mol Med* 31: 437–446.
38. Bayer AS, Eftekhari F, Tu J, Nast CC, Speert DP (1990) Oxygen-dependent up-regulation of mucoid exopolysaccharide (alginate) production in *Pseudomonas aeruginosa*. *Infect Immun* 58: 1344–1349.
39. Leitão JH, Sá-Correia I (1993) Oxygen-dependent alginate synthesis and enzymes in *Pseudomonas aeruginosa*. *J Gen Microbiol* 139: 441–445.
40. Leitão JH, Sá-Correia I (1997) Oxygen-dependent upregulation of transcription of alginate genes *algA*, *algC* and *algD* in *Pseudomonas aeruginosa*. *Res Microbiol* 148: 37–43.
41. Herasimenka Y, Cescutti P, Impallomeni G, Campana S, Taccetti G, et al. (2007) Exopolysaccharides produced by clinical strains belonging to the *Burkholderia cepacia* complex. *J Cyst Fibros* 6: 145–152.
42. Ferreira AS, Leitão JH, Silva IN, Pinheiro PF, Sousa SA, et al. (2010) Distribution of cepacian biosynthesis genes among environmental and clinical *Burkholderia* strains and role of cepacian exopolysaccharide in resistance to stress conditions. *Appl Environ Microbiol* 76: 441–450.
43. Inhülsen S, Aguilar C, Schmid N, Suppiger A, Riedel K, et al. (2012) Identification of functions linking quorum sensing with biofilm formation in *Burkholderia cenocepacia* H111. *Microbiolgyopen* 1: 225–242.
44. Muir ME, van Heeswyck RS, Wallace BJ (1984) Effect of growth rate on streptomycin accumulation by *Escherichia coli* and *Bacillus megaterium*. *J Gen Microbiol* 130: 2015–2022.
45. Sawers RG (1991) Identification and molecular characterization of a transcriptional regulator from *Pseudomonas aeruginosa* PAO1 exhibiting structural and functional similarity to the FNR protein of *Escherichia coli*. *Mol Microbiol* 5: 1469–1481.
46. Fazli M, Bjarnsholt T, Kirketerp-Møller K, Jørgensen B, Andersen AS, et al. (2009) Nonrandom distribution of *Pseudomonas aeruginosa* and *Staphylococcus aureus* in chronic wounds. *J Clin Microbiol* 47: 4084–4089.
47. Römmling U, Fiedler B, Bosshammer J, Grothues D, Greipel J, et al. (1994) Epidemiology of chronic *Pseudomonas aeruginosa* infections in cystic fibrosis. *J Infect Dis* 170: 1616–1621.
48. Götschlich A, Huber B, Geisenberger O, Togl A, Steidle A, et al. (2001) Synthesis of multiple *N*-acylhomoserine lactones is wide-spread among the members of the *Burkholderia cepacia* complex. *Syst Appl Microbiol* 24: 1–14.
49. Clark DJ, Maaloe O (1967) DNA Replication and Division Cycle in *Escherichia Coli*. *Journal of Molecular Biology* 23: 99–112.
50. Huber B, Riedel K, Hentzer M, Heydorn A, Götschlich A, et al. (2001) The *cep* quorum-sensing system of *Burkholderia cepacia* H111 controls biofilm formation and swarming motility. *Microbiology* 147: 2517–2528.
51. Savoia D, Zucca M (2007) Clinical and environmental *Burkholderia* strains: biofilm production and intracellular survival. *Curr Microbiol* 54: 440–444.
52. Fazli M, O'Connell A, Nilsson M, Nichaus K, Dow JM, et al. (2011) The CRP/FNR family protein Bcam1349 is a c-di-GMP effector that regulates biofilm formation in the respiratory pathogen *Burkholderia cenocepacia*. *Mol Microbiol* 82: 327–341.
53. Schmid N, Pessi G, Deng Y, Aguilar C, Carlier AL, et al. (2012) The AHL- and BDSF-dependent quorum sensing systems control specific and overlapping sets of genes in *Burkholderia cenocepacia* H111. *PLoS One* 7: e49966.
54. Schwyn B, Neillands JB (1987) Universal chemical assay for the detection and determination of siderophores. *Anal Biochem* 160: 47–56.
55. Agnoli K, Schwager S, Uehlinger S, Vergunst A, Viteri DF, et al. (2012) Exposing the third chromosome of *Burkholderia cepacia* complex strains as a virulence plasmid. *Mol Microbiol* 83: 362–378.
56. Pessi G, Ahrens CH, Rehrauer H, Lindemann A, Hauser F, et al. (2007) Genome-wide transcript analysis of *Bradyrhizobium japonicum* bacteroids in soybean root nodules. *Mol Plant Microbe Interact* 20: 1353–1363.
57. Yoder-Himes DR, Chain PS, Zhu Y, Wurtzel O, Rubin EM, et al. (2009) Mapping the *Burkholderia cenocepacia* niche response via high-throughput sequencing. *Proc Natl Acad Sci U S A* 106: 3976–3981.
58. Delmotte N, Ahrens CH, Knief C, Qeli E, Koch M, et al. (2010) An integrated proteomics and transcriptomics reference data set provides new insights into the *Bradyrhizobium japonicum* bacteroid metabolism in soybean root nodules. *Proteomics* 10: 1391–1400.
59. Chambers MC, Maclean B, Burke R, Amodei D, Ruderman DL, et al. (2012) A cross-platform toolkit for mass spectrometry and proteomics. *Nat Biotechnol* 30: 918–920.
60. Elias JE, Gygi SP (2007) Target-decoy search strategy for increased confidence in large-scale protein identifications by mass spectrometry. *Nat Methods* 4: 207–214.
61. Qeli E, Ahrens CH (2010) PeptideClassifier for protein inference and targeted quantitative proteomics. *Nat Biotechnol* 28: 647–650.
62. Schrimpf SP, Weiss M, Reiter L, Ahrens CH, Jovanovic M, et al. (2009) Comparative functional analysis of the *Caenorhabditis elegans* and *Drosophila melanogaster* proteomes. *PLoS Biol* 7: e48.
63. Stachel SE, An G, Flores C, Nester EW (1985) A Tn3 *lacZ* transposon for the random generation of beta-galactosidase gene fusions: application to the analysis of gene expression in *Agrobacterium*. *EMBO J* 4: 891–898.
64. Pfaffl MW (2001) A new mathematical model for relative quantification in real-time RT-PCR. *Nucleic Acids Res* 29: e45.